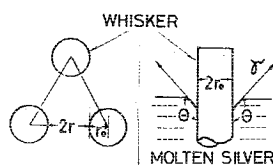
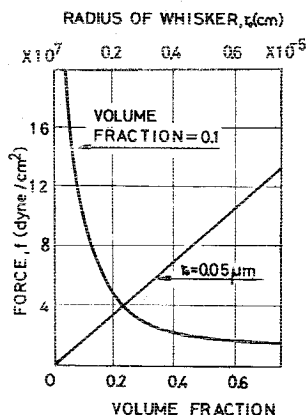


Fig. 2 Configuration of whiskers.

Fig. 3 Dependence of force f on volume fraction v and the thickness of the whisker r .

where r_0 is the radius of the whisker. When we put the volume fraction as v , Eq. (1) can be rewritten as

$$f = -(2v\gamma\cos\theta/r_0) \quad (2)$$

Accordingly, it is sufficient to apply pressure larger than f in order to push voids out of the molten metal.

Figure 3 shows the relation between calculated f values and the volume fraction of whiskers v from Eq. (2) at $\gamma = 890$ dyne/cm, $\theta = 120$ deg, $r_0 = 0.05$ μm and another relation between f and r_0 at $v = 10\%$. The required pressure becomes smaller as the thickness of the whiskers increases. When the thickness of the whisker r_0 becomes larger than $1\mu\text{m}$, the effect of variation in thickness of the whisker on the pressure becomes smaller. It can be found from the equation that the required pressure is about 20 kg/cm^2 at the volume fraction of 10% . Such a degree of pressure can be gained by use of spring. Moreover, it is possible to insure the strength of the sample ampoule shown in Fig. 1 up to about 1000°C by using silica.

Melting Experiment

The samples were heated in the multipurpose electric furnace on Skylab to over 960.8°C , the melting point of silver. However, it was confirmed by ground-based experiments that the samples became molten by heating the furnace up to 990°C and keeping it there for a certain period, because the samples were enclosed triply with graphite sheath, silica tube, and stainless cartridge. Thus the samples were heated at 1010°C for about 4 h to reach a completely molten state. How heating temperature and time affect the properties is not clear. In this experiment, the graphite sheath reacted with the samples, and the surfaces of the samples were partially contaminated. Also, one of the graphite sheaths cracked, and a part of the molten sample flew out of it, and so the effect of pressure on the sample decreased.

In the ground-based tests to establish the temperature condition of the Skylab experiment, the longitudinal axes of sample and sample ampoule were held vertical to the ground, and the piston rod was kept downward to the sample in the furnace. The samples were used for comparison with the low-g samples.

Evaluation Test

The low-g samples were recovered on the ground and examined with respect to density, microstructure, whisker

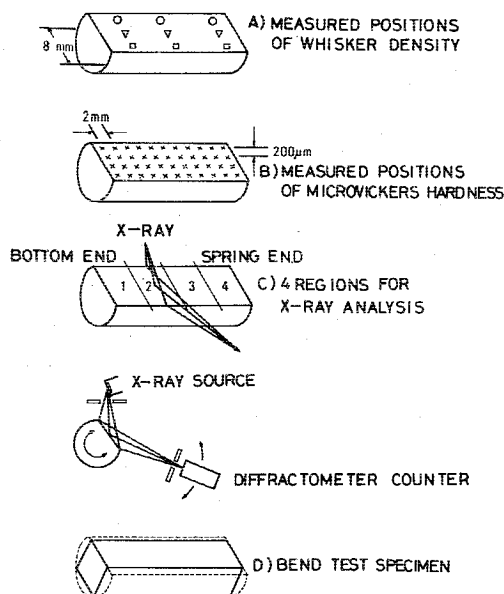


Fig. 4 Experimental procedure.

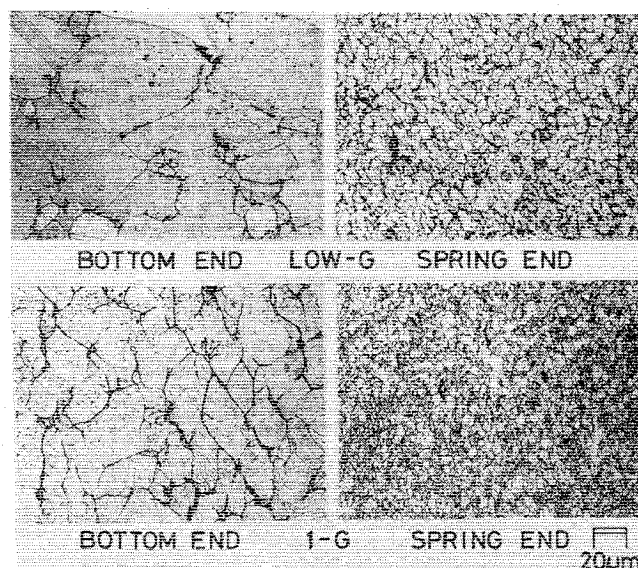


Fig. 5 Photomicrographs of low-g and 1-g samples, Ag-2%SiC.

distribution, x-ray structure, microhardness, bend test strength, fractograph, and so on by the procedure shown in Fig. 4.

III. Experimental Results

Density of Samples

It was recognized that the piston mechanism in the ampoule had worked without any trouble. The ratios of measured density to theoretical ones were about 95% for the low-g samples Ag-2% SiC and Ag-5% SiC. These were about 5% larger than those of the green samples. It was difficult to get such a high increase in density by the ordinary hot press without damaging the whiskers. The density ratio of low-g sample Ag-10% SiC did not increase because of the crack at carbon sheath compared with the density ratio of about 90% for green material. The density increase of 1-g samples had a tendency similar to that of low-g ones.

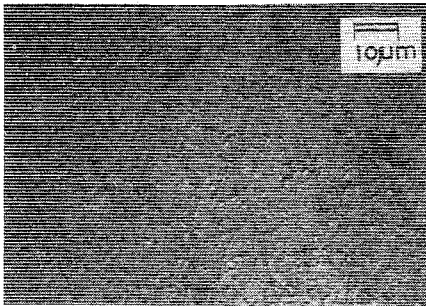


Fig. 6 Photomicrograph showing whisker distribution of low-g sample, Ag-2%SiC.

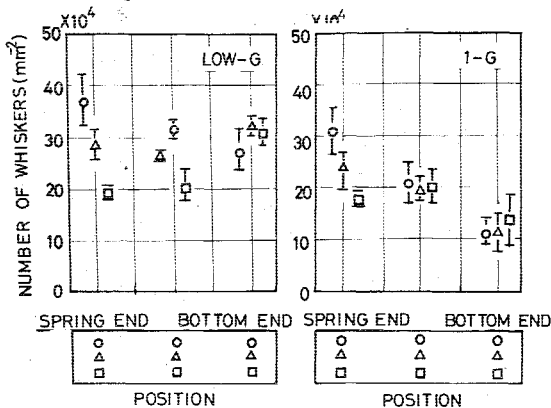


Fig. 7 Distribution density of whiskers, Ag-2%SiC.

Microstructure

Low-g and 1-g Ag-2%SiC samples were etched by 30% aqueous solution containing equivalent volume of ammonium hydroxide and hydrogen peroxide for about 10 s, and microstructures were observed as shown in Fig. 5. These microstructures show a remarkable difference in grain size between spring end and bottom end. The fine grain at the spring end became larger close to the bottom end; moreover, it changed distinctly to a large grain at the middle of the samples. Such a tendency was observed both in low-g samples and in 1-g ones. The temperature characteristic of multipurpose electric furnace and heat through the piston rod seems to be the cause of this phenomenon.

The grain size of low-g samples is larger than that of 1-g samples because of differences in the multipurpose electric furnace soaking condition. The low-g samples were soaked at 1010°C for 4 h, whereas the 1-g ones were soaked at 990°C for 2.5 h. Here the temperature does not indicate that of the samples themselves but rather the sample ampoule cartridges in the multipurpose electric furnace.

Whisker Distribution Density

The cut section as shown in Fig. 4 was observed with a microscope, and the distribution density of whiskers was measured at the different positions of the section. Figure 6 shows the microstructure of low-g sample Ag-2%SiC which was used for the measurement of whisker distribution density.

Using the photomicrographs, the distribution of whiskers was measured by counting the spots that appeared to be whisker sections. The average numbers per unit area and the standard deviation were calculated and plotted corresponding to measurement positions, as shown in Fig. 7. From Fig. 7, it was found that the densities of whiskers in low-g samples were slightly larger than those of the 1-g samples which had the same percentage of SiC as low-g samples, and the decrease of density toward the bottom end along the axial direction as observed in the 1-g samples was not recognized in the low-g samples.

X-Ray Analysis

The x-ray diffraction intensity was measured by an x-ray diffractometer at the four regions of the sample as shown in Fig. 4. The entrance angle of the x-ray and the direction of diffraction also are shown in the same figure. Cu K α radiation was used for diffraction. Figure 8 and Table 1 present the x-ray diffraction data of low-g samples Ag-2%SiC and Ag-10%SiC. There were remarkable differences between low-g samples and 1-g ones in the patterns of x-ray diffraction intensity from the Ag matrix. These patterns represent the distribution of crystallographic planes parallel to the measured surface. The 1-g samples showed random distribution of crystal orientation similar to the calculated value; on the other hand, the low-g samples generally show peculiar patterns. That is to say, the (200) diffraction is unusually strong at region 1 (the bottom side of the sample) of low-g sample Ag-2%SiC, and the (311) diffraction is very strong at regions 1 and 2 of low-g sample Ag-10%SiC. Such peculiarity diminished at regions 3 and 4 (the spring side of the sample) of both samples. These results show that the crystal grains of the solidified silver matrix of low-g samples are not oriented randomly but have a specific orientation. It is more intensive at the opposite side of the piston rod, where it is far from the heat sink, and it is easy to cause the delay of solidification at the comparably high temperature. Regions 1 and 2 correspond to the positions where the large grain was observed.

Assuming that the surrounding thermal condition during solidification was almost the same for both low-g samples and 1-g ones, it seems that the solidification behavior of the silver matrix was different because agitation to thermal convection and flow whiskers did not exit in a weightless environment. This environment presumably was favorable for the growth of columnar texture with a certain preferred orientation in the low-g samples.

Microhardness

The microhardnesses of samples were measured at 2-mm intervals in the longitudinal direction and at 200- μ m intervals in the transverse direction under 100 g of load, as shown in Fig. 4. The results of low-g sample Ag-2%SiC are summarized in Fig. 9, with those of 1-g samples for comparison. They are shown in histograms that vary as the frequency of measurement values. The microhardness for 1-g samples shows a large fluctuation. It is found that the values of microhardness for 1-g samples are very scattered, and the numbers at the maximum frequencies vary like a wave along the longitudinal direction of the samples as compared with

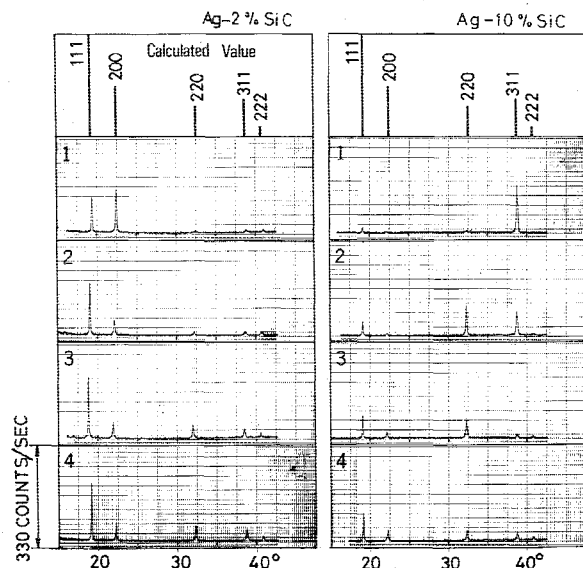


Fig. 8 X-ray diffraction lines for Ag matrix of low-g samples.

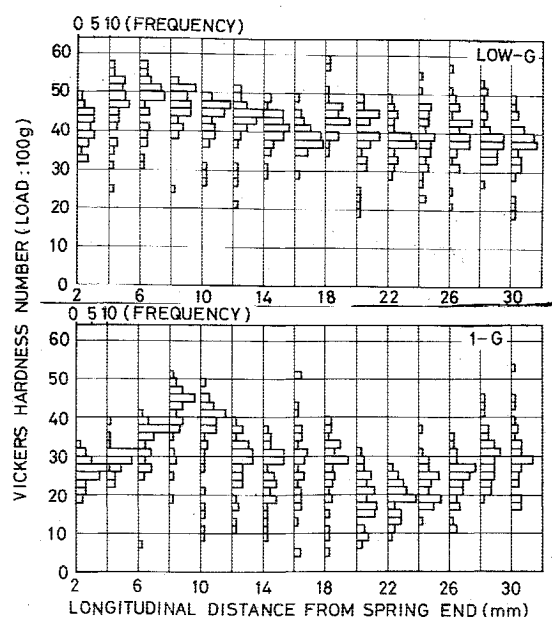


Fig. 9 Histogram showing the distribution of hardness on the section of low-g and 1-g samples, Ag-2%SiC.

low-g samples. Similar results also are recognized in Ag-5%SiC and Ag-10%SiC samples.

Bend Test

The specimens for bend tests were cut from both Ag-5%SiC and Ag-10%SiC of low-g and 1-g samples using a diamond saw and shaped as shown in Fig. 4. The tests were carried out by a three-point bending method using an Instron-type tensile testing machine equipped with a loading adapter, as shown in Fig. 10.

The length of the specimens was 3.0-3.5 cm, the width b , 4-5 mm, and the thickness t 3-4 mm. The curvature of tips of the two edges for supporting the sample was 2.5 mm in radius, and the distance between their edges l_0 was 25 mm. The curvature of the loading edges was 12.5 mm in radius. The applied load was measured with an electric load cell. The deflection at the loading point was measured as the displacement of crosshead of the testing machine, because it was connected directly to the loading adapter. The crosshead speed was kept constant at 0.19 mm/min during the test.

Load-deflection curves are shown in Figs. 11 and 12. These figures indicate that the deformation behavior on bending is distinctly different between low-g and 1-g samples. Namely, 1-g specimens revealed almost totally elastic deformation and

Fig. 10 Instrument for bend tests.

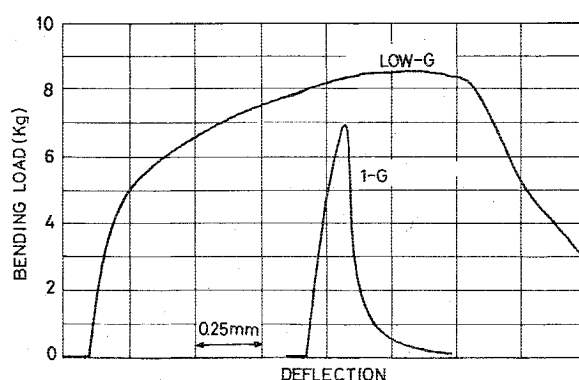
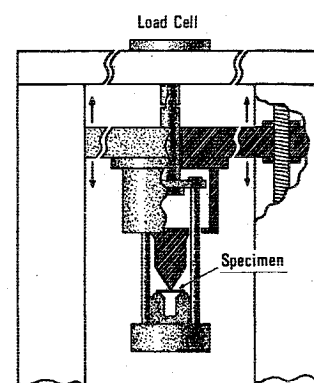


Fig. 11 Load deflection curves in bend test for low-g and 1-g samples, Ag-5%SiC.

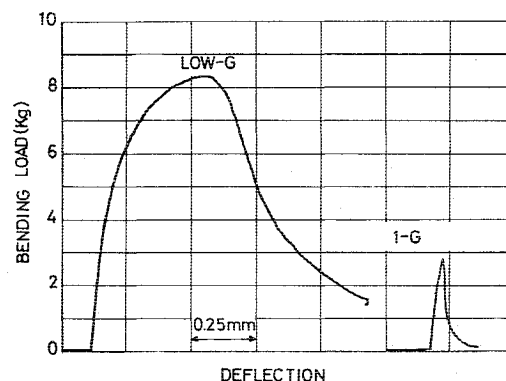


Fig. 12 Load-deflection curves in bend test for low-g and 1-g samples, Ag-10%SiC.

Table 1 X-ray diffraction intensity from Ag matrix for low-g and 1-g samples

| Relative intensity calculated | Measured position | Peak diffraction intensity (counts/s) from lattice plane (hkl) | | | | |
|-------------------------------|-------------------|--|-------|-------|-------|-------|
| | | (111) | (200) | (220) | (311) | (222) |
| 1-g sample, Ag-2%SiC | 1 | 400 | 110 | 80 | 70 | 20 |
| | 4 | 380 | 120 | 107 | 73 | 20 |
| low-g sample, Ag-2%SiC | 1 | 117 | 147 | 3 | 7 | 8 |
| | 2 | 177 | 53 | 13 | 12 | 10 |
| | 3 | 213 | 53 | 43 | 27 | 15 |
| | 4 | 193 | 63 | 50 | 43 | 15 |
| low-g sample, Ag-10%SiC | 1 | 17 | 3 | 7 | 160 | 2 |
| | 2 | 43 | 5 | 97 | 80 | 2 |
| | 3 | 83 | 20 | 67 | 13 | 7 |
| | 4 | 97 | 37 | 30 | 27 | 10 |

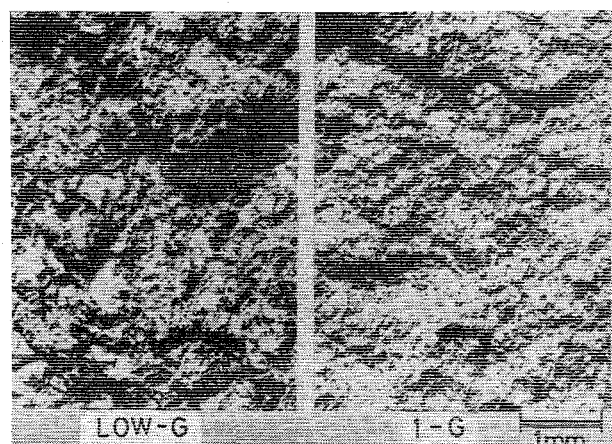


Fig. 13 Fractographs showing general view of fractured surfaces for low-g and 1-g samples. Ag-5%SiC.

cracked on the lower surface with a small amount of deflection, and then fractured. On the other hand, the low-g specimens revealed a large amount of deflection due to plastic deformation, and then cracked on the lower surface. It is considered that the cracks occurred in the lower surface of the specimen at the maximum loading point in the load-deflection curve.

From the preceding results, the tensile stress at the lower surface corresponding to the maximum point of the load-deflection curve was calculated as the bend strength σ_f . The calculated values of σ_f are listed in Table 2. They were calculated for 1-g specimens by Eq. (3) assuming that the fracture occurred in the elastic region, and for the low-g specimens by Eq. (4) assuming that the fracture occurred after overall plastic deformation;

$$\sigma_f = 3/2 (l_0/bt^2) P_{\max} \quad (3)$$

$$\sigma_f = (l_0/bt^2) P_{\max} \quad (4)$$

Here l_0 is the length of span between the supporting edges, and P_{\max} is the maximum load.

Observation of Fractured Surface

Low-magnification photographs of fractured surfaces after bend tests are shown in Fig. 13. Larger steps or ledges are observed for the low-g samples compared with the 1-g samples. Scanning electron micrographs also were taken for the purpose of examining the fractured surfaces in more detail. The representative ones are shown in Figs. 14 and 15. The lower surfaces were selected as the observation positions because the parts where cracks occurred seem to be the most important. The characteristic features of the low-g and 1-g specimens are different from each other. The fractured surfaces of the low-g specimens show dimple patterns, which

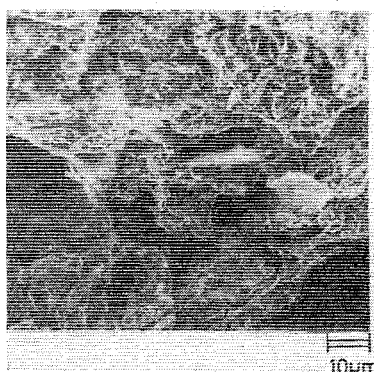


Fig. 14 Scanning electron microphotograph of the fractured surface for low-g sample. Ag-5%SiC.

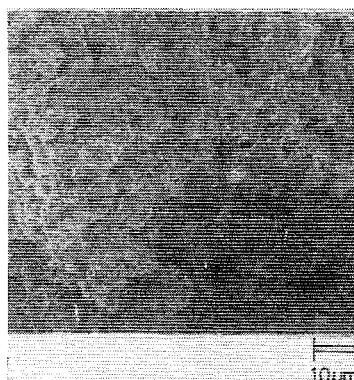


Fig. 15 Scanning electron microphotograph of the fractured surface for 1-g sample. Ag-5%SiC.

is characteristic of ductile fracture, whereas those of the 1-g specimens reveal spongelike or gravel-like structures with very few dimples.

IV. Considerations

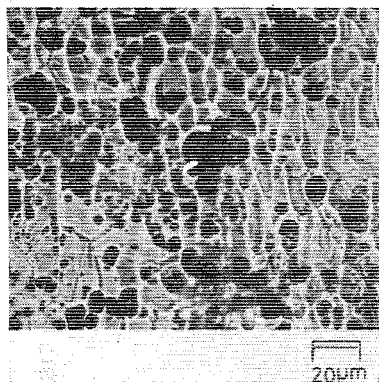
The thermometer in the multipurpose electric furnace recorded 1010°C, and it also was confirmed by the observation of low-g samples recovered on the ground that they had been in a molten state. However, it was not certain whether or not the temperature distribution of the samples in a molten state had been uniform. Judging from the construction of the electric furnace and the sample ampoule, the photomicrographs of the sample's surfaces as shown in Fig. 16, and the preferred orientation of the low-g samples, it is considered that there was a certain temperature gradient that was lower toward the piston rod side at the solidification. This tendency also can be observed in Fig. 5.

The photomicrostructures as shown in Fig. 6 were used to obtain the results of Fig. 7. The distribution density of whiskers was measured by counting the spots that appeared to be whisker sections. In this case, the counted numbers of whiskers depended on the resolving ability in the microscope and photographic conditions, because the diameters of whiskers were not constant but varied over a wide range

Table 2 Results of bend tests for low-g and 1-g samples, Ag-5%SiC, Ag-10%SiC

| | | low-g samples | | 1-g samples | |
|--|----------------------------------|---------------|-----------|-------------|-----------|
| | | Ag-5%SiC | Ag-10%SiC | Ag-5%SiC | Ag-10%SiC |
| Volume fraction of whiskers, % | | 5 | 10 | 5 | 10 |
| Dimension of test specimens | Width b , mm | 5.20 | 4.04 | 4.66 | 4.17 |
| | Thickness t , mm | 3.30 | 3.89 | 3.57 | 4.15 |
| Length of span between supports l_0 (mm) | | 25 | | | |
| Maximum load | P_{\max} (kg) | 8.5 | 8.3 | 7.0 | 2.8 |
| Bend strength | σ_f (kg/mm ²) | 3.7 | 3.4 | 4.4 | 1.5 |
| Mode of fracture | | Ductile | | Brittle | |

Fig. 16 Photomicrograph of surface of low-g sample, Ag-10%SiC.



around a mean diameter of $0.1 \mu\text{m}$. Accordingly, these measured distribution densities are to be regarded only to indicate relative values.

Here we should notice that the effect of whiskers on the solidification texture of matrix silver was proved by x-ray analysis. We do not expect the second phase to contribute measurable effects to the crystal orientation of silver. In fact, x-ray analysis of 1-g samples showed usual x-ray patterns of polycrystallized silver which accorded with the calculated results. The fact that the preferred orientation changed to either (311) or (200) according to the contents of whiskers appears to prove a certain contribution of silicon carbide whisker to the solidification texture of silver. Assuming that the simple mixing of two phases obliges the solidification process to change, it will be an interesting theme in the future.

The configuration in the distribution of whiskers, the structure of matrix silver, and so on are well reflected in the experimental results of bend tests and hardness. The clear distinction in mechanical properties between the low-g samples and the 1-g ones seems to testify to the following facts. The microscopic segregation of whiskers strongly occurred during the melting process in the 1-g samples, in addition to macroscopic segregation.

Contrary to this, it is presumed that no such segregation of whiskers as to stress concentration existed in the low-g samples. Therefore, the low-g specimens were fractured by bend loading after fully plastic deformation of the silver matrix. The ultimate tensile strengths σ_f for low-g samples Ag-5%SiC and Ag-10%SiC are considered to be almost the same as that of the silver matrix itself, since the amount of whiskers was relatively small.

In the case of the 1-g samples, the local segregation of whiskers resulted in the formation of spots or zones that were rich with whiskers. At the region where whiskers were richest, the silver matrix became porous after solidification and sometimes solidified as independent small particles. It was recognized by scanning electron micrographs that these coarse structure regions must have acted as the crack initiation sites and caused early brittle fracture in the 1-g samples.

V. Conclusions

1) The experiments were performed to process the composite materials, which consisted of a silver matrix and silicon carbide whisker of 2, 5, and 10% volume, as a strengthening material by melting and pressurizing in the multipurpose electric furnace on Skylab.

2) The sample ampoules designed to give molten material a pressure operated successfully and the density ratio largely increased in both samples of low-g and 1-g.

3) Crystal grain sizes of low-g and 1-g samples at the spring end were about one-tenth of those at the other end because of the influence of the structure of the sample ampoule and the temperature characteristic of the multipurpose electric furnace.

4) Although the samples consisted of two materials having great differences in densities and were kept in a molten state for over 4 h, a trend of separating whiskers from silver was not observed in the low-g samples but was observed macro- and microscopically in the 1-g samples, which were kept in a molten state for less than 2 h.

5) From the measurements of microhardness and distribution density of whiskers, the low-g samples showed uniform hardness and uniform distribution of whiskers all over them. The whiskers of the 1-g sample were distributed richly at the spring end compared to the other end, and the values of hardness were scattered widely with their measured positions.

6) From the x-ray analysis, it was found that matrix silver of low-g samples was a solidified structure showing clearly preferred orientation. Such orientation was in the region of large grain. However, the x-ray diffraction patterns for matrix silver of 1-g samples were similar to those of ordinary silver.

7) The results of bend tests showed that the low-g samples did not exhibit brittle fracture, which was a characteristic of 1-g samples, but rather large ductility.

8) The preceding results indicate clearly that the low-g samples were devoid of influences of floating due to the density difference and thermal convection; accordingly, the low-gravity environment is a preferable place where the high-quality composite materials can be well processed.

Acknowledgments

The author would like to express his sincere appreciation to NASA and particularly to the staff at the Marshall Space Flight Center for their cooperation and enthusiastic support during the M-561 experiment. He is especially indebted to W. R. Adams and I. C. Yates for their many efforts during all phases of the experiment, and to M. P. L. Siebel and H. F. Wuenschel for their great encouragement in carrying out the experiment. The author also is grateful to T. Araki and S. Yoshida of the National Research Institute for Metals for their encouragement throughout this work, to the Science and Technology Agency of the Japanese Government and T. Kawada for their support, and to T. Hoshi for preparing of sample ampoules.

References

- ¹ Levitt, A. P., ed., *Whisker Technology*, Wiley, New York, 1970, p. 443.
- ² Takahashi, S. and Suzuki, T., "Preparation of Whisker Reinforced Metal Composites and Their Properties," *Composite Materials and Structures*, Vol. 2, Jan. 1973, p. 22.
- ³ Gnesin, G. G. and Nayditch, Y. V., "Contact Reaction of Silicon Carbide with Molten Copper," *Powder Metallurgy*, Feb. 1969, p. 57.
- ⁴ Takahashi, S. and Kuboi, O., to be published by *Journal of Materials Science*.